# DUAL MODALITY TOMOGRAPHY: THE IMAGE ANALYSIS OF FORWARD PROBLEM

RASIF MOHD ZAIN[1*], RUZAIRI ABDUL RAHIM[2]
& SITI ZARINA MOHD MUJI[4]

**Abstract**. The paper presents the novel idea in process tomography which is the combination of dual modality; electrical capacitance and optical tomography for monitoring solid/gas flow measurement. Dual Modality Tomography (DMT) system consists of eight electrodes of capacitance sensor and 16 pairs of optical sensor in one sensor plane. The data obtained from both sensors were inseries transfer to PC with control and triggered by data acquisition system. The data obtained from both sensors will then be reconstructed into image using Linear Back Projection or Iterative Reconstruction Algorithm. In this project, the DMT produces an image fusion, which is developed based on the adjustment of pixel values and the detection region of pixel images reconstruction between capacitance and optical tomography sensor. Series of error analyses will determine the feasibility of the DMT sensors to perform as an instrument in solid flow visualization.

*Keywords*: Electrical capacitance tomography; optical tomography; dual mode tomography; image fusion; reconstruction algorithm

**Abstrak.** Kertas kerja ini mempersembahkan satu idea yang baru di dalam proses tomografi iaitu kombinasi di antara dua modaliti; *electrical capacitance* dan optikal tomografi untuk mengawasi pengukuran aliran pepejal/gas. Sistem *Dual Modality Tomography* (DMT) mengandungi lapan sensor *capacitance* elektrod dan 16 pasang sensor optikal di dalam satu lapis sensor. Data yang diambil dari kedua-dua sensor dipindahkan sesiri ke PC dengan kawalan dan dipicu oleh sistem perolehan data. Data yang didapati daripada kedua-dua sensor akan distrukturkan semula kepada imej menggunakan *Linear Back Projection* atau *Iterative Reconstruction Algorithm*. Di dalam projek ini, DMT akan menghasilkan cantuman imej, yang mana dibangunkan berdasarkan penyesuaian nilai pixel dan kawasan pengesanan pada penstrukturan semula imej pixel di antara sensor *capacitance* dan optikal tomografi. Senarai analisis kesilapan akan menentukan kebolehlaksanaan sensor DMT untuk menentusahkan ia sebagai instrumen bagi melihat aliran pepejal.

*Kata kunci*: *Electrical capacitance* tomografi; optikal tomografi; dua mod tomografi; cantuman imej; algoritma penstrukturan semula

---

[1] Malaysian Nuclear Agency (Nuclear Malaysia)
[2] Department of Control and Instrumentation, Faculty of Electrical Engineering,
Universiti Teknologi Malaysia, 81310 UTM Johor Bahru, Johor Darul Ta'azim, Malaysia
[3] Faculty of Electrical and Electronic Engineering, Universiti Tun Hussein Onn Malaysia,
86400 Parit Raja, Batu Pahat, Johor
* Corresponding author: rasif@nuclearmalaysia.gov.my

## 1.0   INTRODUCTION

Numerous types of tomography sensors have been designed and given attention in monitoring and investigating the industrial solid/gas flow. This research was carried out in order to obtain the quality of cross-sectional image in for the industrial needs which will benefit financially to the plant. However, though many researches have been done in this field, they remain as notorious task.

Several sensing principles of tomography are used to produce image on solid/gas flow, such as the electrical capacitance, gamma, and optical tomography which considered as of one tomography modality [1]. Obviously, in the previous researches, the use of one tomography modality is not capable to gain a high-resolution image in full range distribution, and not sufficient to explore all important flow characteristics [1]. Currently, the new trend in sensor development of solid/gas flow is either through dual or triple modality in one sensor plane. This technique enables to overcome the constraints found when one tomography modality is applied. Table 1 below shows the advantages and limitations of sensing modalities from previous numerous researches.

**Table 1**  The advantages and limitation of tomography modalities in solid/gas flow measurement

| Sensing Principle | Advantages | Limitations |
|---|---|---|
| Electrical capacitance | Low cost, no radiation, rapid response and robustness [1, 3, 6], full concentration distribution [2], temporal resolution [3] | Blurred image in low concentration distribution below < 30% [2, 5], soft-field sensing where low image resolution 0.2% for a single object when near the wall of the pipe. 2% at the centre of the pipe [2], image reconstruction complicated [1] |
| Optical | Spatial resolution 2% [2, 5], good measurement in medium distribution and content in whole investigate cross section simultaneously [7,11], safe and free of electromagnetic interference [7], low cost | Limited measurement in high distribution flow above 35% [2,] |
| Gamma ray | Spatial resolution 1% [3, 4] | Require relatively long time for energy integration, mechanical movement to obtain of the whole region [7, 4], radiation dose to the surrounding [3, 4], heavy shielding [4] |

*Continued* **Table 1**

| Sensing Principle | Advantages | Limitations |
|---|---|---|
| Dual mode; Electrical capacitance & gamma | High spatial & temporal resolution image [3, 4, 10]. | Radiation dose to the surrounding [3, 4], heavy shielding [4,], high cost. |

Thus, as a conclusion considering the limitations of sensing principle, a new idea is presented through developing a dual mode tomography system which combines an electrical capacitance and optical sensor in one sensor plane. The performance of the system in forward problem is discovered and investigated in this research.

## 2.0   THEORETICAL CONSIDERATION

In this project the sensor is based on hard-field and soft-field techniques. A hard-field system like the optical tomography is equally sensitive to the parameter it measures in all positions throughout measurement volume [4]. Meanwhile, for the soft-field sensors, like capacitance tomography, are sensitive to the measured parameter depending on the position in the measurement volume. In a dual mode system however, different sensors often provide some complementary process information [4]. The optical output signals from the circuit are proportional to the received light, which means a higher flow volume will results in a lower output signals. Meanwhile the capacitance output signals are proportional to the dielectric material, which means a higher flow volume will results in a high output signals.

An imaginary image plane consisting of $32 \times 32$ pixels is drawn using the device-context object, which encapsulates the Windows APIs for drawing lines, shapes, and text.  The actual flow area is being identified. All calculations or pixel scanning are done in the range of this identified area instead of the whole area of $32 \times 32$ pixels. This step does not only save the computation time but also minimizes the usage of the computer resources.

The predicted output sensor values are being generated after selecting several pixels to represent certain phantom object's surface. The DMT image fusion is generated based on this assumption:

i.    Both of the sensitivity maps of sensors are equal in grid square resolution. i.e. $32 \times 32$.

ii.   The $C_i(\Delta T)$ defines the temporal material concentration for the *ith* pixel of a pipe cross section at a time interval $\Delta T$. Let $p_i^{\,O}(\Delta t)$ defines corresponding pixel value into reconstructed image from data captured by optical sensor and $p_i^{\,C}(\Delta t)$ define the data captured by electrical capacitance

sensor. Therefore both of this sensors are good in temporal resolution, $C_i(\Delta T) = p_i^O(\Delta t) = p_i^C(\Delta t)$.

ii.    The threshold level distribution ($L$) for capacitance tomography, $L = 35\%$. Value of $L$ is based on the maximum distribution of optical tomography.

iii.   The detect regions (area) is the image fusion derived through the adjustment of the pixel values $p_i^C$. Where the concentration is lower $p_i^C \leq L$, $p_i^C$ is not taken into consideration of the $P^F ith$ account and in turn the $P^F ith = p_i^O$ is applied. Meanwhile for $p_i^O \geq L$ the ith pixels follow the $P^F ith = p_i^C$. Let $P_{i,j}^F$ represents the pixel values in final frame. The individual pixel $P_{i,j}^F$ from $n$ final frame must meet the condition

$$\sum_{j=1}^{n} P_{ij}^F = \begin{cases} \sum_{j=1}^{n} p_{ij}^C \subseteq L = \sum_{j=1}^{n} p_{ij}^O \\ \sum_{j=1}^{n} p_{ij}^O \supseteq L = \sum_{j=1}^{n} p_{ij}^C \end{cases}$$

(Equation 1)

where, $n$ the number of frame, $i$ the number of pixel, $j$ the number of frames, $P^F ith$ defines corresponding pixel in image fusion, $p_i^O$ is pixel value for optical tomography and $p_i^C$ is pixel value for capacitance tomography.

The electrical capacitance sensor's reconstructed image represents capacitance distribution in a pipe cross-section and normalized concentration distribution $c$, $0 \leq c \leq 1$ in full range distribution. Meanwhile, the reconstructed image from the optical sensor represents a normalized intensity distribution, respectively, $0 \leq O \leq 1$ below threshold ($L$) distribution. Figure 2 shows the flow chart representing the steps involved in the algorithm while Figure 1 shows the mainframe of the forward modeling GUI.
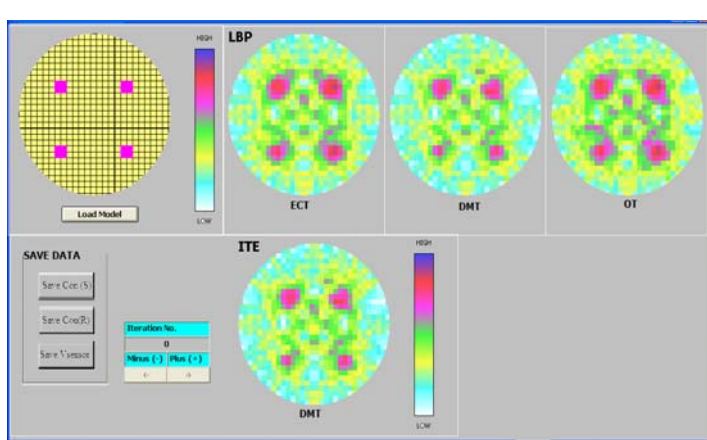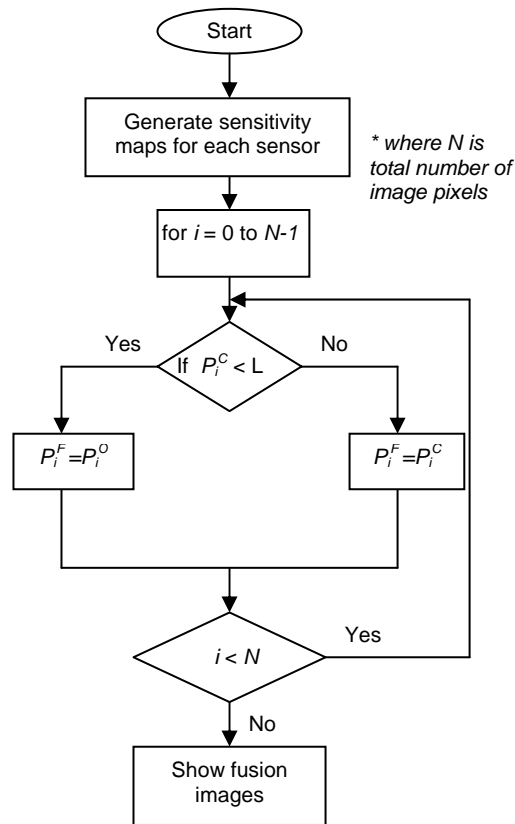


**Figure 1**  GUI modeling

**Figure 2** Flow chart for image fusion

## 3.0   IMAGE QUALITY ANALYSIS

Abdul Rahim (2008) mention in his work that the simulation of an artificial flow regime is aimed to synthetically examine the reconstructed image and computational cost by analyzing state space error [5]. Besides, this act also allows the running time of the reconstruction process to use the Linear Back Projection (LBP) Algorithm and Iterative Reconstruction Algorithm (IRA) respectively. Image quality can be defined in general terms as an indicator of the relevance of the information presented by an image to the task we seek to accomplish using this image [6]. Ideally, the reconstructed image should be identical to the standard image (true distribution of object) but in practice differences arose due to limitations of the image reconstruction algorithms.

The error theory in measurement science that can be used to evaluate the discrepancy between the reconstructed and the standard/original image is peak signal to noise ratio or **PSNR**. PSNR is calculated by the following formula in Equation 2 [7].

$$PNSR = 10\log_{10}\left(\frac{f(x,y)_{max}^{2}}{\frac{1}{n^{2}}\sum_{x=0}^{n-1}\sum_{y=0}^{n-1}\left[f(x,y)-f_{A(x,y)}\right]^{2}}\right) \text{dB} \qquad \text{(Equation 2)}$$

where

$f(x,y)_{max}$    = the maximum value of the entire image

$f_{A}(x,y)$     =     reconstructed image

$n^{2}$    = image size

In general, the higher value of PSNR, the higher the quality of an image. If two images are identical, the PSNR would be infinite. This is because the ratio of Signal to Noise is higher. Here the 'signal' is the original image and the 'noise' is the error in reconstruction [8]. The actual value of the PSNR is not meaningful, but the comparison between two values for different reconstructed images gives one measure of quality. All the calculations for the error analyses are being implemented using Visual Basic programming.

## 4.0   STATIC DISTRIBUTION FLOW MODEL

The experiment for static distribution flow model is based on time independent. In order to test the performance of **DMT** system in high spatial resolution a single object flow model is tested. The expected result for the **DMT** will be able to present and measure a small diameter object.

For single object flow model, a small size object is selected. The diameter of object is measured by using the electronic digital caliper. The size of object is converted to the number of pixels according to the scale of the image plane in forward modeling. Equation 3 presents the formula to convert from mm to pixel numbers.

$$n_{pixels} = \left(\frac{Total pixel Sensitivity maps}{diameter of sensor}\right) * D_{mm}$$

(Equation 3)

where, total pixel is 1024
　　　　diameter = 100 mm
　　　　$n_{pixels}$ = number of pixels
　　　　$D_{mm}$ = measured object (mm)

The property of the object is tabulated in Table 2. The selected of objects in round shape because it resembles the shape of the plastic beads that used in industrial purpose.

**Table 2**  Phantom properties

| Single Object | Shapes | Diameter (mm) | Object Diameter (pixel) | Object Area (pix²) |
|---|---|---|---|---|
| Wire -wrap | Round | 0.45 | 2.88 | 26 |

The DMT tomograms for the modeled images are generated by predicting the sensor values during object disruption and also using the LBP and iterative algorithms. For iteration reconstruction algorithm it is developed in a range starting from 0 to 15.  For zero iteration represents the result of LBP algorithm, and at the same time verifies that the iterative reconstruction algorithm can only be obtained after the LBP algorithm is implemented. In other words, the iterative reconstruction algorithm is the further process of the LBP algorithm data.

The image analysis of PSNR errors between the offline reconstructed image and the original modeled image are being analyzed. In this research the maximum number of iteration is set at the $15^{th}$ iteration. Besides the tomogram for true distribution of the object, the color bar represents the color scale for the density of tomogram; with 'LOW' representing low density and 'HIGH' representing high density of the image.

## 5.0   RESULT AND DISCUSSION

From the experiment results of the image is shown in Figure 3, with the processed PSNR error data of ECT, OT and DMT in linear back projection algorithm are tabulated in Table 3.
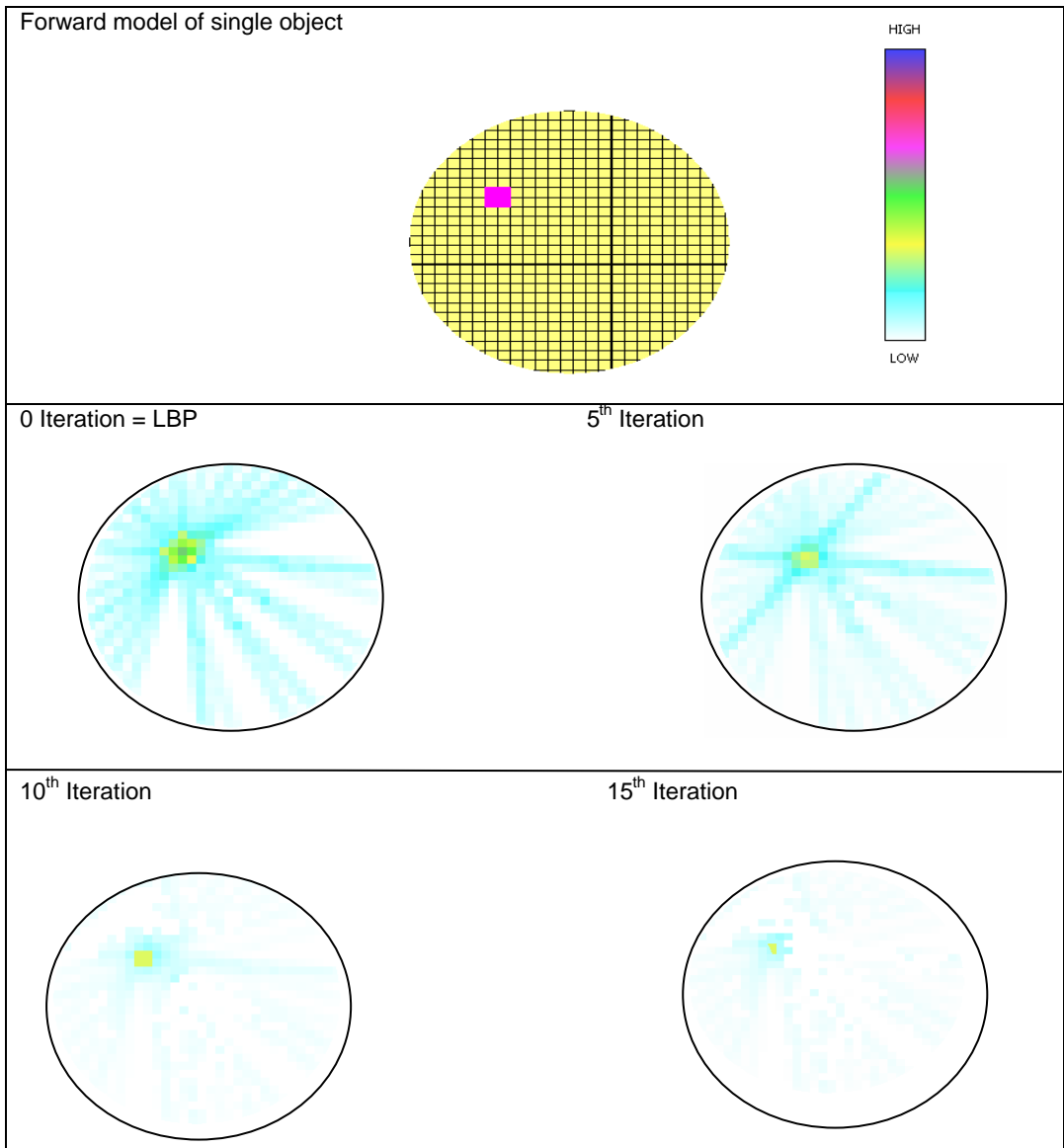
**Figure 3**  Tomograms for single object

**Table 3**  PSNR result analysis of different sensor

| Type of Sensor | PSNR (dB) |
|----------------|-----------|
| ECT | 43.89 |
| DMT | 49.22 |
| OT | 45.72 |

In the results shown, it can be interpreted that the DMT provides a good quality image compared to the OT and ECT. The DMT provides the best image quality where PSNR slightly higher by 10.82% compared to the ECT and 7.11% by OT. The image fusion of DMT is a good spatial resolution compared to a single modality. From this result also OT provides a good quality image compared to the ECT. Figure 4 shows the performance of image fusion compared to a single modality.
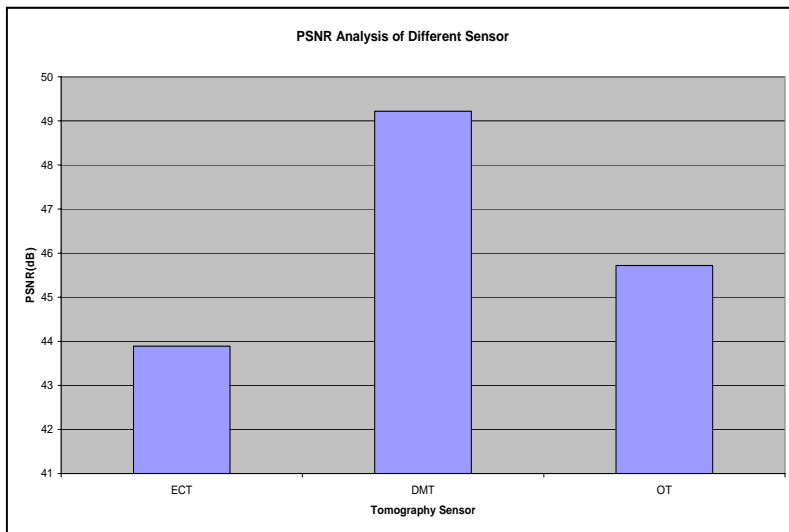


**Figure 4**  PSNR analysis of different sensor

In order to get the best quality image for DMT, the number of iteration should be selected based on the PSNR analysis. The PSNR error data of DMT image reconstruction in different iteration is shown in Table 4.

**Table 4**  PSNR result analysis for DMT

| No. of Iteration | PSNR (dB) |
| :---: | :---: |
| 0 (LBP) | 49.22 |
| 1 | 49.73 |
| 2 | 49.89 |
| 3 | 49.92 |
| 4 | 49.98 |
| 5 | 50.09 |
| 6 | 50.12 |
| 7 | 50.19 |
| 8 | 50.25 |
| 9 | 50.37 |
| 10 | 50.45 |
| 11 | 50.39 |
| 12 | 50.31 |
| 13 | 50.24 |
| 14 | 50.11 |
| 15 | 49.99 |

Single objects with a diameter of 0.45 mm are traced whereby zero iteration or the LBP image shows the lowest PSNR. As the iterative reconstruction algorithm is being implemented, the increment from the first iteration to the $10^{th}$ iteration results the PSNR  increased to the maximum value. After the $10^{th}$ iteration, the PSNR values decreased all the way to the $10^{th}$ iteration. The result is true with the statement made by Liu (2004) which says that after a certain number of iterations, the fidelity of the images starts to deteriorate constantly [9]. The PSNR Analysis with different iteration is shown in Figure 5.

## 6.0   CONCLUSION

To prove the ability of DMT as a good sensor compared to single modality, the quality image analysis have been done. The analysis is based on forward problem where a single model has been selected. The data from PSNR, error measurement have been manipulated and interpreted due to show that the DMT is good compared to the single modality. For a good image reconstruction of DMT, the IRA analysis has been made and the best number of iteration has been selected.
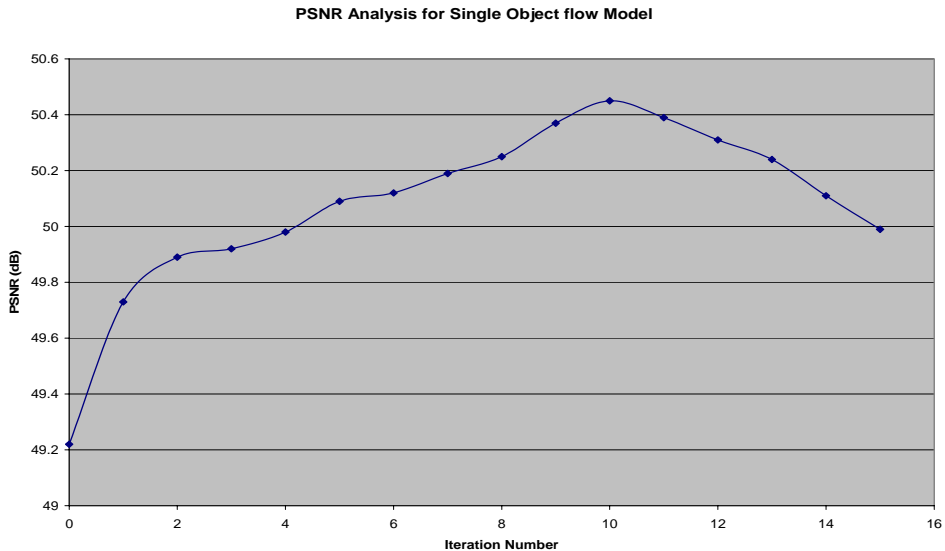
**Figure 5** PSNR analysis with different iteration

## ACKNOWLEDGMENTS

## REFERENCES

[1]     R. Abdul Rahim, Chiam, K.T., Jayasuman, P. 2009. Embedded System Based Optical Tomography: The Concentration Profile. *Sensor Review Journal.* 29(1): 54-62.

[2]     R. G. Green, R. Abdul Rahim, K. Evans, F. J. Dickin, B. D. Naylor, T. P. Pridmore. 1998. Concentration Profiles in a Gravity Chute Conveyor by Optical Tomography Measurement. *Powder Technology Journal.* 49-54.

[3]     W. Q. Yang, S. Liu. 2000. Role of Tomography in Gas/solid flow Measurement. *Flow Measurement and Instrumentation.* 237-244.

[4]     G. A. Johansen, T. Froystein, B. T. Hjertaker, O. Olsen. 1996. A Dual Sensor Flow Imaging Tomographic System. *Meas. Sci. Technol.* 297-307.

[5]     Abdul Rahim, R., L. C. Leong, K. S. Chan, J. F. Pang. 2008. Hardware Implementation of Multiple fan Beam Projection Technique in Optical Fibre Process Tomography. *Sensor Journal.* 8: 3406-3428.

[6]     Abdou, I. E. and Dusaussoy, N. J. 1986. Study on Image Quality Measurements. Newark: IEEE. 71-78.

[7]     R. Abdul Rahim and Chan Kok San. 2008. Optical Tomography Imaging in Pneumatic Conveyor. *Sensors & Transducer Journal (IFSA)*. 95(8). 40-48.

[8]     L. C. Leong, R. Abdul Rahim, K. S. Chan, M. H Rahiman and J. F. Pang. 2008. Real Time Mass Flow Rate Measurement Using Multiple Fan Beam Optical Tomography. *ISA TRANSACTIONS.* 47(1): 3-14.

[9]     Liu, S. Fu, L. Yang, W. Q. Wang, H G. Jiang, F. 2004. Prior-Online Iteration for Image Reconstruction with Electrical Capacitance Tomography. 195-200.

[10]    M. R. Rzasa. 2009. The Measuring Method for Tests of Horizontal Two-Phase Gas-Liquid Flows, Using Optical And Capacitance Tomograph. *Nuclear Engineering and Design*. 239(4): 699-707.

[11]    C. Yan, *et al*. 2005. Design of An Applied Optical Fiber Process Tomography System. *Sensors and Actuators B: Chemical*. 104(2): 324-331.